Kinetic Analysis of Oxygen Utilization during Cofactor Biogenesis in a Copper-Containing Amine Oxidase from Yeast†

Benjamin Schwartz, Joanne E. Dove, and Judith P. Klinman*

Departments of Chemistry and Molecular and Cell Biology, University of California, Berkeley, California 94720

Received September 24, 1999; Revised Manuscript Received January 12, 2000

ABSTRACT: A detailed kinetic analysis of oxygen consumption during TPQ biogenesis has been carried out on a yeast copper amine oxidase. O_2 is consumed in a single, exponential phase, the rate of which responds linearly to dissolved oxygen concentration. This behavior is observed up to conditions of maximally obtainable oxygen concentrations. In contrast, no viscosity effect is observed on rate, implicating a high K_m for O_2. Binding of oxygen appears to occur faster than its consumption and to result in displacement of the precursor tyrosine onto copper to form a charge-transfer species, described in the the preceding paper of this issue [Dove, J. E., Schwartz, B., Williams, N. K., and Klinman, J. P. (2000) *Biochemistry 39,* 3690-3698). Reaction between this intermediate and O_2 is proposed to occur in a rate-limiting step, and to proceed more rapidly when the tyrosine is deprotonated. This rate-limiting step in cofactor biogenesis does not display a solvent isotope effect and is, thus, uncoupled from proton transfer. Comparisons are drawn between the proposed biogenesis mechanism and that for the oxidation of reduced cofactor during catalytic turnover in the mature enzyme.

Copper-containing amine oxidases (CAOs)[1] are a class of enzymes which catalyze the two electron oxidative deamination of amines, producing ammonia and hydrogen peroxide:

$$RCH_2NH_3^+ + O_2 + H_2O \rightarrow RCHO + NH_4^+ + H_2O_2 \quad (1)$$

The biological roles of these enzymes may be as diverse as the number of organisms in which they can be found; in bacteria, CAOs allow amines to be used as a source of carbon and nitrogen for growth, while in plants, these enzymes are integrally involved in developmental processes and wound healing (*1*, *2*). In mammals, CAOs are found in a variety of organs, such as the kidney, blood serum, high endothelial venules (HEVs) of the lymph nodes, and various ocular tissues, among others (*3*, *4*). Functions for these enzymes have been proposed to involve the detoxification and regulation of biogenic amines and the production of hydrogen peroxide as a possible cell signaling agent (*1*). Recently, chronic diabetic disorders such as nephropathy, retinopathy, and neuropathy have been linked to the activity of CAOs. It is thought that the production of some aldehydes from biogenic amines, such as formaldehyde and methylglyoxal, as well as the production of hydrogen peroxide can accelerate nonspecific protein modification and agglutination, resulting in microvascular damage to various organs (*5*). The potential to alleviate these chronic conditions makes CAOs an attractive target for pharmaceutical investigation (*6*).

The redox cofactor in all CAOs studied to date has been shown to be 2,4,5-trihydroxyphenylalanine quinone (TPQ) (*7*, *8*). TPQ is formed by posttranslational modification of a specific tyrosine residue[2] within the protein's structure (*9*). This transformation requires only copper and oxygen; no additional enzymes or cofactors are needed (*10*, *11*). A detailed mechanism has been postulated for TPQ biogenesis (Scheme 1), based largely on chemical intuition and inferences drawn from several crystallographic studies (*12*). However, to date, there has been no corroborative measure of this mechanism, either by identification of intermediates or by detailed kinetic measurements.

In this study, we present the first detailed kinetic analysis of oxygen utilization during TPQ biogenesis in an amine oxidase from *Hansenula polymorpha* (HPAO). Several new mechanistic features have been revealed by this approach: a specific oxygen binding site is implicated, and the overall rate-limiting step is concluded to be reaction of O_2 with the precursor tyrosine, which is activatied via formation of a charge-transfer complex with copper. Similarities and differences between this biogenesis mechanism and the catalytic oxidative half-reaction are discussed.

EXPERIMENTAL SECTION

Mutagenesis, Expression, and Protein Preparation for Metal-Free HPAO. The mutants N404D and E406Q used

† This work was supported by a National Institutes of Health Grant to J.P.K. (GM 39296). Benjamin Schwartz was supported by a National Institutes of Health Postdoctoral Fellowship (GM 18813). J.E.D. was supported by a training grant from the National Institutes of Health (GM 08295-10).

* To whom correspondence should be addressed. E-mail: klinman@socrates.berkeley.edu. Phone: (510) 642-2668. Fax: (510) 643-6232.

[1] Abbreviations: CAOs, copper-containing amine oxidases; TPQ, 2,4,5-trihydroxyphenylalanine quinone; DPQ, 3,4-dihydroxyphenylalanine quinone; HPAO, *Hansenula polymorpha* amine oxidase; BSAO, bovine serum amine oxidase; AGAO, *Arthrobacter globiformis* amine oxidase; PCD, protocatechuate 3,4-dioxygenase; PCA, protocatechuate; CT, precursor tyrosine-copper charge-transfer species.

[2] Apo-enzyme refers to metal-free, TPQ-free protein. In the apo-enzyme, the tyrosine which is converted to TPQ (Y405 in HPAO) is referred to as the precursor tyrosine or Y405.

10.1021/bi9922244 CCC: $19.00
Published on Web 03/09/2000

Scheme 1: Previously Proposed Biogenesis Mechanism (adapted from ref *12*)

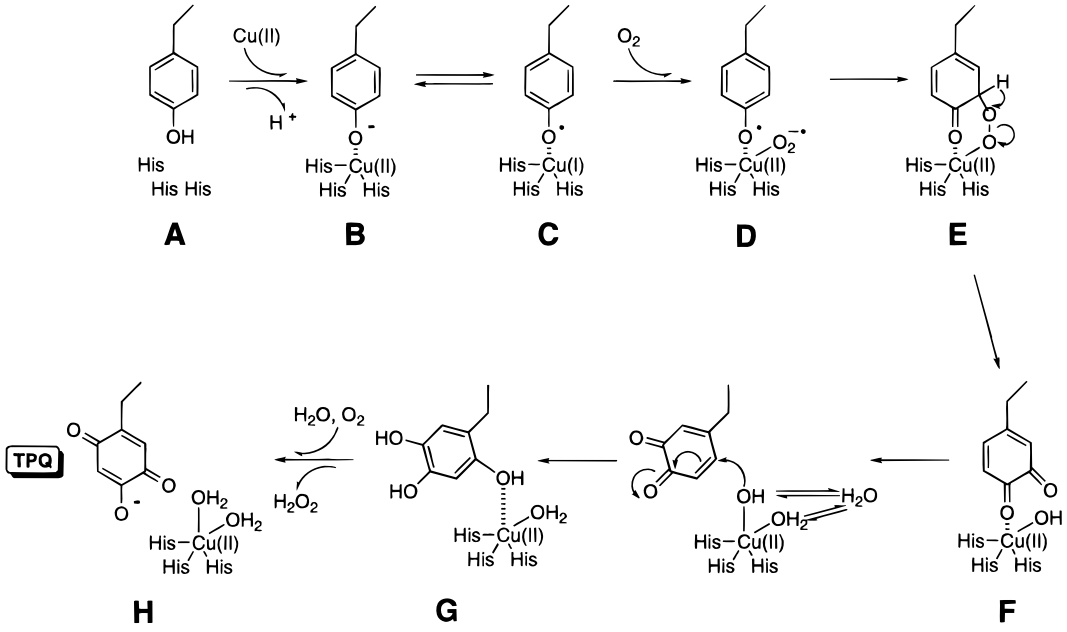

in this study were obtained as described previously (*13*). Metal-free WT and mutant proteins were obtained by growing *Escherichia coli* transformed with the appropriate pET11a-derived pKW3 expression vector in media prewashed with chelex resin, to which copper chelators were added at the point of induction, as described previously (*14*). Protein used for solvent isotope studies was dialyzed versus deuterated buffer (HEPES, 50 mM, pD = 7.4) as a final step. The concentrations of proteins were determined by Bradford analysis (Bio-Rad) using bovine serum albumin as a standard.

Buffer Preparation. Except for assays varying in pH (or pD), all reactions were done in HEPES, pH 7.0, ionic strength = 50 mM. Different buffers were used in various pH regimes, in accordance with their buffering ranges; MES (50 mM) was used for pHs 6.0 and 6.5, HEPES (50 mM) was used for pHs 7.0, 7.5, and 8.0, and CHES (50 mM) was used for pHs 8.5 and 9.0. Each buffer was adjusted to an ionic strength of 50 mM with the addition of the appropriate amount of potassium chloride.

Buffers of different viscosities were prepared by the addition of varying amounts of glycerol to buffer (HEPES, pH 7.0, or CHES, pH 8.6). The relative viscosity ($\eta/\eta°$) of each solution was determined relative to buffer alone at 25° using an Ostwald-type capillary viscometer (Fisher Scientific). The dissolution of glycerol at a concentration of 253.5 g/L led to a $\eta/\eta° = 1.53$ at pH 7.0 and 1.55 at pH 8.6, while glycerol at 391.5 g/L led to a $\eta/\eta° = 2.20$ at pH 7.0 and 2.22 at pH 8.6.

Buffers at various pDs were prepared by dissolving the appropriate salt in D_2O (Cambridge Isotope Labs, 99.9%), followed by adjustment of the pD by NaOD. The pD was calculated by adding 0.4 to the pH meter reading (*15*).

Calibration of Oxygen Electrode. Because O_2 concentrations vary with changes in percent viscosogen and temperature, it was necessary to recalibrate the electrode when varying either parameter. To accomplish this, buffer was equilibrated for 20 min under new conditions, after which a baseline was collected and the scale was set to 100.0%. Following this, the consumption of oxygen during the turnover of protocatechuic acid (PCA) by protocatechuate 3,4-dioxygenase (PCD) was measured as described previosuly (*16*); this reaction is known to consume 1 mol of oxygen/1 mol of substrate, and the extinction coefficient for both substrate (PCA) and product (β-CM) are known (*16*). After complete depletion of substrate, the concentration of O_2 was determined by dividing the amount of substrate consumed by the change in oxygen scale, to yield an effective concentration of dissolved oxygen under a given set of conditions.

Measurement of Oxygen Consumption. All reactions were carried out on a Clark oxygen electrode (YSI model 5300). The total volume was 1.0 mL, consisting of 970−975 μL of buffer and 25−30 μL of apo-enzyme (~10 μM final concentration in assay). For each biogenesis measurement, the buffer was allowed to equilibrate for 15−20 min before apo-enzyme was added. To change the concentration of oxygen, a mixture of O_2 and N_2 (varying in ratio) was blown over the solution during buffer equilibration. After apo-enzyme was added and a baseline was collected, 1 equiv of copper chloride was added to initiate biogenesis, and the exact concentration of O_2 was recorded.

UV−Vis Spectroscopy. UV−vis spectra were obtained on a HP8452A diode-array spectrophotometer (Hewlett-Packard) fitted with a constant-temperature bath. The appearance of TPQ was followed at 480 nm, where the ϵ_{max} is equal to 2000 M^{-1} cm^{-1} (*1*). Reactions monitored in this manner were 150 μL total volume, consisting of apo-protein (at 40 μM final concentration) in Hepes (50 mM, pH 7.0). Biogenesis was initiated either by addition of copper or by introduction of O_2. To initiate with copper, 1 equiv of $CuCl_2$ was added to an aerobic sample of apo-protein. To initiate with O_2, a sample of apo-protein was placed in an anaerobic cuvette and flushed with argon (bubbled through a basic solution of pyrogallol) for 1 h. A solution of $CuCl_2$ was similarly made anaerobic. 1 equiv of copper was then added via airtight syringe, and the reaction was followed until no absorbance changes were observed, ~15 min (*13*). Subsequently, bio-

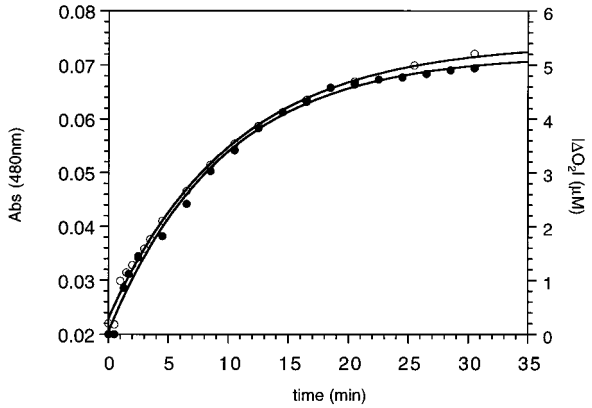

FIGURE 1: Time course of TPQ formation and O_2 consumption. TPQ formation (○) was followed spectrophotometrically at 480 nm in 50 mM HEPES, pH 7.0, at 25 °C. O_2 consumption (●) was observed in a Clark oxygen electrode under similar buffer conditions. The data for both reactions are fitted with a single-exponential function.

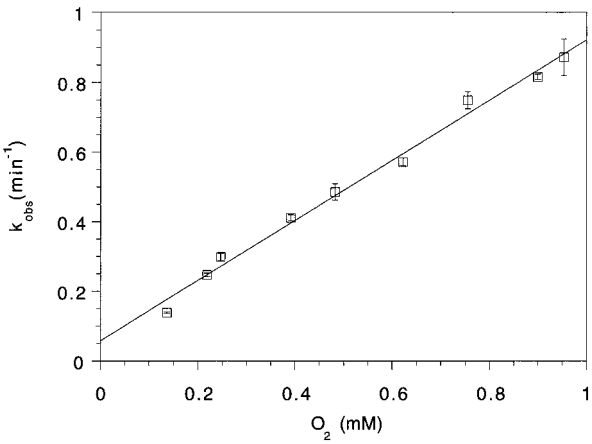

FIGURE 2: Response of observed rate of O_2 consumption (k_{obs}) to oxygen concentration. k_{obs} was measured at various concentrations of dissolved O_2, from 0.15mM up to 1mM (in 50 mM HEPES, pH 7.0, 25 °C). The slope, generated by a linear fit of the data, is the second-order rate of biogenesis, k_{bio}.

genesis was initiated by rapid aeration of the protein. Similar procedures have been reported by this lab (*17*).

Data Fitting. Both O_2 consumption and TPQ formation were fitted to a single-exponential function with nonlinear regression analysis provided by the program Kaleidagraph. The errors from these fits were used for subsequent calculations of k_{bio} under various conditions. To fit the data in Figure 4, the following equation was used:

$$k_{bio} = k_{bio(low\ pH)}/(1 + 10^{(pH-pK)}) + k_{bio(high\ pH)}/(1 + 10^{(pK-pH)})$$

In Table 1, the minimally detectable signal was calculated based on an estimated lower limit of observable O_2 consumption (nmol O_2/min) divided by the amount of enzyme used:

$$k_{obs}\ (\text{minimal}) = (0.24\ \text{nmol}\ O_2/\text{min})/\text{nmol apo-protein}$$

RESULTS

Relative Rates of Copper Binding, Oxygen Consumption, and TPQ Biogenesis. The rates of biogenesis initiated with either copper or oxygen were investigated. To initiate with copper, metal was added to an aerobic sample of apo-enzyme; initiation with oxygen was carried out by aerating a sample of apo-enzyme, which had been preincubated anaerobically with copper. With either method, the observed rates (k_{obs}) were virtually indistinguishable (Figure 1).

The relative rates of oxygen consumption and TPQ biogenesis were determined under similar conditions for WT protein and two mutants, N404D and E406Q (Table 1). With

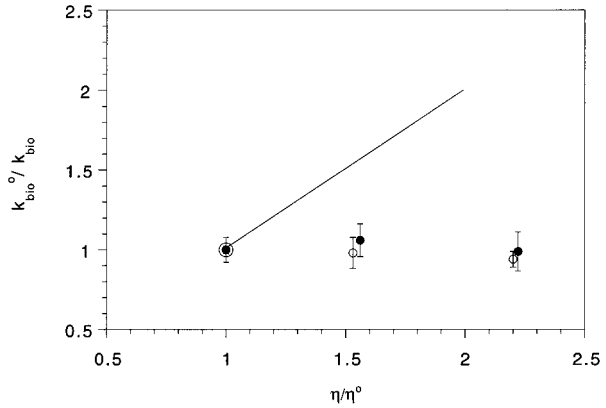

FIGURE 3: Effect of solvent viscosity on k_{bio}. Relative rates of biogenesis ($k_{bio}°/k_{bio}$) were determined in solvents with relative viscosities ($\eta/\eta°$) equal to 1.00, 1.53, and 2.20 at pH 7.0 (○), and 1.00, 1.56, and 2.22 at pH 8.6 (●). The expected response of a diffusion-controlled reaction is shown as a straight line.

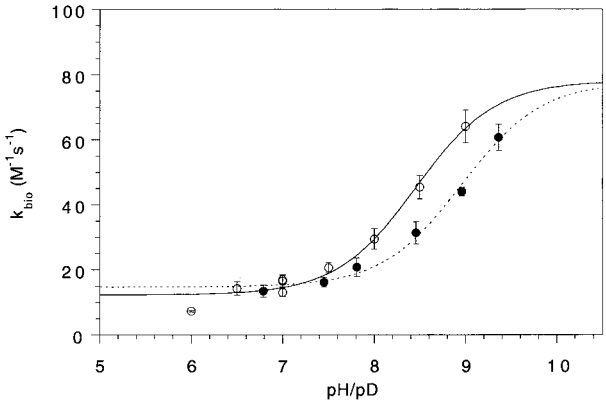

FIGURE 4: Effect of pH and solvent isotope on k_{bio}. k_{bio} was determined in buffers varying in either pH (○) or pD (●). The data were fit to a function with differing rates at low and high pH/pD. The value is equal to 12 M^{-1} s^{-1} at low pH and 78 M^{-1} s^{-1} at high pH, with a pK of 8.45. The value at low pD is equal to 14 M^{-1} s^{-1} and 78 M^{-1} s^{-1} at high pD, with a pK of 8.95.

Table 1: Kinetics of TPQ Formation and Oxygen Consumption[a]

	k_{obs} (min^{-1})		
	TPQ formation[c]		O_2 consumption
	initiated with Cu(II)	initiated with O_2	initiated with Cu(II)
WT HPAO	0.08 ± 0.03	0.08 ± 0.03	0.10 ± 0.03
E406Q	0.013 ± 0.005	0.017 ± 0.006	0.017 ± 0.005
N404D	0.0006 ± 0.0002	0.0007 ± 0.0002	<0.003[b]

[a] Assays were conducted under ambient oxygen concentrations (250 μM), at 25 °C and in HEPES (pH 7.0, ionic strength = 50 mM). [b] No rate was detected, but an upper limit of 0.003 min^{-1} was estimated based on the minimally detectable signal (see experimental for calculation). [c] Measured at 480 nm. Reported rates are the average of at least three trials.

both WT and E406Q, k_{obs} for oxygen consumption and cofactor formation were nearly identical, despite the nearly 10-fold reduction in each parameter for the mutant relative to WT. In the case of N404D, no oxygen consumption could be detected; an upper limit is estimated based on the limits of detection of the oxygen electrode.

Effect of Varying Oxygen Concentration on the Rate of Oxygen Consumption during Biogenesis. The observed rate of oxygen consumption was followed as a function of varying oxygen concentration under standard conditions (Figure 2). A linear response of k_{obs} was attained up to maximally obtainable O_2 concentrations (~1 mM at 25 °C), and from this, a second-order rate, or k_{bio}, of 14.4 ± 0.5 M^{-1} s^{-1} was calculated. Saturation was not observed for plots under any of the conditions studied herein (see below), where viscosity, pH, solvent isotope, and temperature were varied.

Effect of Viscosity on Biogenesis. Buffers were made at relative viscosities ($\eta/\eta°$) of 1.00, 1.53, and 2.20 at pH 7.0 and 1.00, 1.55, and 2.22 at pH 8.6. The effect of viscosity on k_{bio} can be seen in Figure 3; there is no apparent change in rate at either pH studied.

Effect of pH on Biogenesis. The effect of pH was determined by measuring the change in k_{bio} in buffers ranging from pH 6.0 to 9.0 (Figure 4); buffers outside this range could not be used due to nonspecific protein denaturation. Values for biogenesis of 12.3 ± 1.4 M^{-1} s^{-1} at low pH and 78.1 ± 6.7 M^{-1} s^{-1} at high pH were determined, with a p*K* at 8.45 ± 0.13.

Effect of Solvent Isotope on Biogenesis. The effect of solvent isotope was ascertained by measuring k_{bio} in buffers of varying pD values (Figure 4). A similar response to the profile in protiated buffers was observed, with a k_{bio} of 77.8 ± 7.4 M^{-1} s^{-1} calculated at high pD and 14.7 ± 1.5 M^{-1} s^{-1} at low pD. The p*K* value, however, was shifted approximately 0.5 units to 8.96 ± 0.13.

Effect of pH on Formation of CT Species. The effect of varying pH on the appearance of the CT species was followed spectrophotometrically at 350 nm (*13*). At pH 8.6 (Figure 5A), the CT complex was observed to form to a much greater extent than at pH 7.0 (Figure 5B). In both cases, the disappearance of the 350 nm band appeared to coincide with the formation of TPQ at 480 nm.

Effect of Temperature on Biogenesis. k_{bio} was determined at 20, 25, 30, and 35 °C (Figure 6). From these rates, an Arrhenius plot was constructed (inset) and an enthalpy of activation of 8.4 ± 0.5 kcal/mol was found. This value is much less than the 37.6 kcal/mol[3] found previously for a mutant of the N404 (adjacent to TPQ) position (*18*).

DISCUSSION

Since the discovery of TPQ in 1990 (*7*), the mechanism by which it is formed has remained a compelling question. Initially, it was shown that copper and oxygen are both necessary and sufficient to produce TPQ (*10*). This result, coupled with the fact that the active site contains a mononuclear copper, led to a hypothesis for cofactor formation, the general features of which are shown in Scheme 1 (*12*). Beginning with apo-enzyme (A), copper is bound and

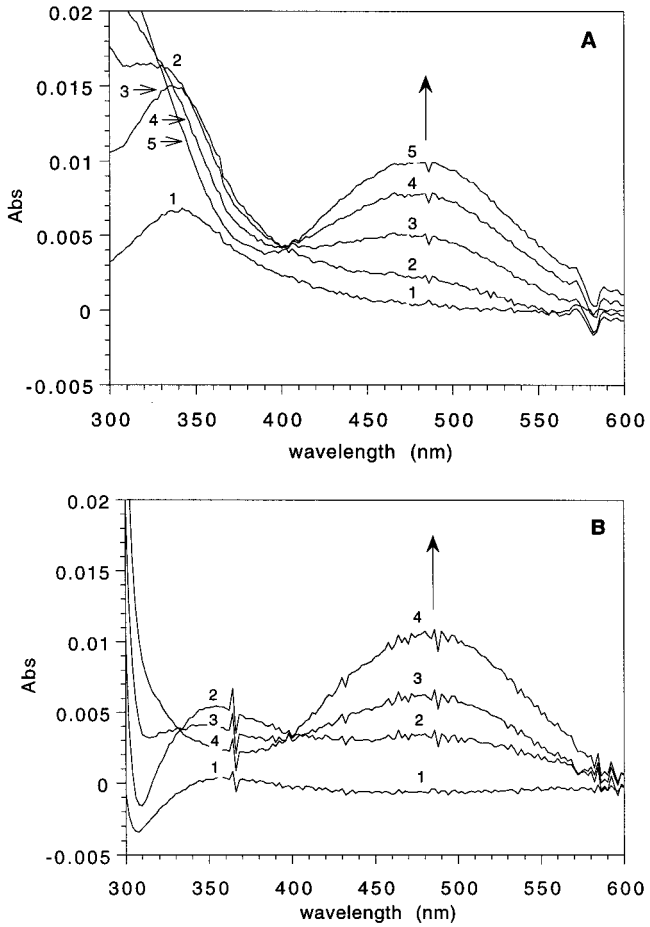

FIGURE 5: Effect of pH on UV−vis spectra of CT species. (A) Apo-HPAO at pH 8.56 was preincubated with Cu(II) anaerobically, until no further absorbance changes were observed (*13*). A baseline spectrum was recorded at this point, followed by rapid aeration of the sample. Displayed spectra are subtractions of the baseline at 1, 3, 5, 7, and 9 min (labeled spectra 1−5, respectively) consequent to aeration. (B) Apo-HPAO was prepared as in panel A, but at pH 7.00. Spectra are subtractions from the baseline at 1, 5, 10, and 20 min consequent to aeration (labeled spectra 1−4, respectively).

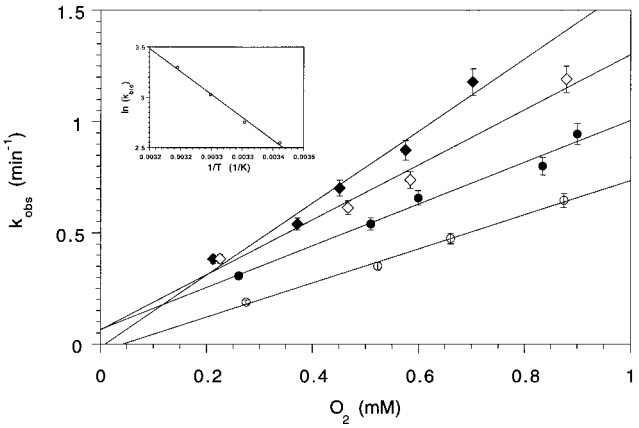

FIGURE 6: Effect of temperature on k_{bio}. k_{obs} was determined at various concentrations of O_2 at 20 °C (○), 25 °C (●), 30 °C (◇), and 35 °C (♦). The fitted Arrhenius plot of k_{bio} is shown in the inset.

subsequently ligands the precursor tyrosine (B) to form an activated complex. This species is proposed to be in equilibrium with tyrosyl radical-Cu(I) (C), formed via electron transfer from the precursor tyrosine to the metal. The equilibrium is believed to largely favor species B

[3] In a previous paper (*18*), the value of $\Delta H^{\ddagger}$ for the biogenesis of N404A was incorrectly reported as 9 kcal/mol due to a calculational error.

because of the inability to detect by EPR any organic radical or reduction of Cu(II) signal when copper is prebound to apo-enzyme anaerobically (*19*). O_2 then diffuses to the active site and reacts with Cu(I) to form Cu(II)-superoxide (D), which subsequently collapses with the tyrosyl radical to form a peroxy intermediate (E). Deprotonation of this intermediate leads to dopa quinone (DPQ) (F). After formation of DPQ, the Michael addition of H_2O or OH^- yields topa (G), which in the final step is reoxidized to the mature, redox-active TPQ (H). The conversion of G to H is also envisioned to contain a realignment of TPQ, such that the C-5 oxygen is oriented toward the active-site copper, in accordance with the structures of mature AGAO and ECAO (*12*).

The credibility of this mechanism rests on crystallographic studies of an amine oxidase from *Arthrobacter globiformis* (AGAO), in which the mature cofactor is seen to access conformations expected to occur during biogenesis, but thought to be nonproductive during turnover (*12*). A crystal structure of the apo-enzyme of AGAO has also been reported, indicating the precursor tyrosine in a position to interact with the vacant copper site (*12*). Additionally, some of the transformations proposed have been shown to occur in model systems. For example, the Michael addition of H_2O/OH^- on DPQ has been shown to occur in solution, as has the reoxidation of the quinol form of TPQ (*20*).

However, there has been no direct evidence supporting the proposal shown in Scheme 1, and many of the specific mechanistic details concerning TPQ formation have remained unclear. For example, the initial reaction of apo-enzyme with O_2 may occur in a diffusional encounter, as with glucose oxidase (*21*), or by prebinding of oxygen to a specific, nonmetal site on the enzyme, as with PCD or CAOs during turnover (*19*, *22*). Also unknown are the factors which influence the formation and breakdown of the tyrosine-Cu(II) CT species (A → B, C → D). The prototropic state of the apo-enzyme, coupling of proton and electron transfer, and positioning effects by active-site residues may all affect these crucial mechanistic steps. To probe these isssues directly, we undertook a detailed kinetic analysis of the consumption of O_2 during TPQ biogenesis in HPAO.

Nature of Rate-Limiting Steps in Biogenesis. We initially turned our attention to the binding of copper. It has been shown that copper is necessary to initiate biogenesis and that no TPQ is generated when other metals such as zinc, cobalt, or nickel are used in its place (*10*, *14*). To determine the kinetic significance of copper binding, biogenesis was initiated either with or without Cu(II) prebound; to initiate with Cu(II) prebound, metal was first added to an anaerobic preparation of protein, followed by rapid aeration to form TPQ. The rates of biogenesis were found to be 0.08 min^{-1} with either method (Table 1), indicating that copper binding is relatively rapid compared with biogenesis. This result is consistent with previous work in AGAO, where it was found that TPQ formation was zero order with respect to metal, in excess of one equivalent (*19*). The effect of copper binding was also determined for E406Q and N404D, mutants which flank the precursor tyrosine (Y405) and are known to play integral roles in controlling the conformation of TPQ during turnover (*18*). With these mutants, copper binding was also found not to affect the overall rate of cofactor formation (Table 1).

As a consequence of the fast apparent rate of copper binding, subsequent experiments were initiated by the addition of metal to aerobic samples. Under these conditions, the consumption of O_2 appeared to coincide with TPQ formation (Figure 1) and to occur in a single-exponential phase. Because these experiments are for a single turnover reaction, two salient mechanstic points can be deduced from this result. First, in light of recent reports which implicate the uptake of 2 equiv of oxygen/TPQ formed (*23*), the course of oxygen consumption shown in Figure 1 indicates that the first O_2 reacts more slowly than the second; a biphasic response in O_2 consumption would have been observed if the first equivalent reacted more quickly. Second, the data in Figure 1 indicate which steps can be rate determining in biogenesis. The similar rate constants for O_2 consumption and TPQ formation signify that a step concurrent with or preceding the reaction of apo-protein with the first equivalent of O_2 is rate limiting. If the mechanism shown in Scheme 1 is correct, this step must be the diffusion-controlled reaction between the metal and dioxygen, since metal binding has already been shown to not affect the overall rate of cofactor formation. To test this possibility, the response of k_{obs} to O_2 concentration was pursued.

The effect of changing O_2 concentration upon k_{obs} is shown in Figure 2; even up to maximally obtainable values of dissolved O_2 (~1 mM at 25 °C and ambient pressure), k_{obs} varies linearly with $[O_2]$, consistent with a diffusion-controlled reaction between apo-HPAO and O_2. The second-order rate constant determined from the slope of this plot is equal to 14.4 ± 0.5 M^{-1} s^{-1} and is referred to as k_{bio}.

The small magnitude of k_{bio} and the absence of saturation in the k_{obs} vs $[O_2]$ plot (Figure 2) presents an apparent contradiction. A lack of curvature in enzyme reaction plots of velocity vs [substrate] is most easily reconciled with a diffusion-controlled process; however, most diffusion-limited enzyme reactions proceed at rates on the order of 10^7-10^9 M^{-1} s^{-1} (*24*). If k_{bio} involves electron transfer or additional chemistry, its magnitude may be small. This has been shown to be the case in glucose oxidase, where the first electron-transfer reaction between reduced flavin and dioxygen occurs at 10^4 M^{-1} s^{-1} at high pH (*21*). Alternatively, the data in Figure 2 may indicate the presence of an oxygen binding site, with an affinity higher than 1 mM. A binding site for oxygen has been shown for another amine oxidase from bovine serum (BSAO) during turnover, with an estimated K_m of ~50 μM (*22*). The apparent weak affinity of HPAO for O_2 during biogenesis could be the result of differential steric effects by the precursor tyrosine and mature TPQ at the O_2 binding site or may be due to other, nonbinding steps in the mechanism as K_m is a kinetic contant derived from k_{cat} and k_{cat}/K_m (*25*). Indeed, the K_m for O_2 during catalysis was found to increase more than 100-fold in a mutant of HPAO due to kinetic considerations (*17*). To discern whether the reaction between apo-enzyme and O_2 is limited by diffusional chemistry or involves specific binding of oxygen, the effect of solvent viscosity was investigated.

Studying an enzyme reaction in buffers of varying solvent viscosity is expected to yield information about the diffusional nature of measured rates (*26*). If the reaction between apo-HPAO and O_2 occurs as a diffusion-limited encounter, as shown in Scheme 1, it is expected that a linear, positive correspondence between the relative reaction rates, k_{bio}°/k_{bio},

and the relative solvent viscosity, $\eta/\eta°$, will be displayed; coversely, a reaction limited by nondiffusion steps will show no dependence. The effect of solvent viscosity on the rate of biogenesis was determined by comparing k_{bio} for reactions run in buffers of varying glycerol content (Figure 3). The rates in the three solvents studied, varying in $\eta/\eta°$ from 1.0 to 2.2, are indistinguishable. This determination was made at both low (7.0) and high pH (8.6), as pH was determined to effect k_{bio} (vide infra). The lack of a discernible viscosity effect implies that oxygen does not react in a diffusion-controlled manner with apo-enzyme as proposed in Scheme 1, but rather oxygen prebinds with a weak affinity to the precursor protein.

This conclusion is also supported by spectroscopic results, which show that there likely exists an intermediate formed during biogenesis which is oxygen dependent, but occurs before O_2 is consumed (*13*). On the basis of its λ_{max} and kinetic profile, the intermediate is proposed to be a tyrosine-copper charge transfer (CT) species. It is important to note that in H624C the data imply saturation by oxygen under ambient conditions ($\sim$250 μM) in order to yield an equivalent of the CT species (*13*), whereas the kinetic results shown in Figure 2 for WT HPAO suggest a K_m for O_2 of >1 mM. The different behavior of H624C and WT is likely the result of the several order of magnitude difference in their rate of breakdown of the CT complex to yield TPQ, i.e., a kinetically complex K_m for O_2 during biogenesis.

From the kinetic evidence presented herein and the spectroscopic data in the following paper in this issue (*13*), it appears that oxygen not only binds to a specific site on the apo-enzyme, but that this binding event causes a displacement of the precursor tyrosine onto the copper. Further, the observation that the CT species forms faster than O_2 is consumed argues that the formation of the precursor tyrosine−Cu(II) complex is not rate-limiting in biogenesis; if this were the case, the appearance of the CT species would occur concomitant with reaction with dioxygen.

The movement of Y405 associated with O_2 binding may account for the relatively high K_m for oxygen, as the coupling of the two processes is expected to lower the on-rate for O_2. This contention is supported by work in PCD, in which the oxygen-binding site is partially occluded by an active-site tyrosine axially liganded to Fe(III) in the resting enzyme. Substrate binding triggers displacement of the axial tyrosine, revealing the binding site for O_2; when this tyrosine was mutated to a histidine, which could not ligand the active-site Fe(III), the K_m for oxygen decreased significantly, presumably due to an increased on-rate as a result of uncoupling of O_2 binding from the associated conformational encumberances (*27*).

After probing the nature of oxygen binding, we turned our attention to the effect of pH on k_{bio}. Insofar as crucial active-site residues can be titrated, the pH profile for biogenesis should yield information about the active prototropic state of the apo-enzyme. The effect of changing pH on k_{bio} is shown in Figure 4. There are two distinct rates observed, with values of 78.1 M^{-1} s^{-1} at high pH and 12.3 M^{-1} s^{-1} at low pH and a p*K* of 8.45. On the basis of its value, the observed p*K* may reasonably be assigned to the precursor tyrosine; though 8.45 is lower than the pK_a for free tyrosine ($\sim$10), it is quite similar to p*K*s found for active-site tyrosines in Fe-containing superoxide dismutase, human aldose reductase, and glutathione S-transferase (*28*−*30*). Ideally, the origin of a kinetically determined p*K* should be definitively established by direct titration of the corresponding residue. However, this determination cannot be done for Y405 in apo-HPAO because the large number of tyrosines and tryptophans in the protein preclude direct spectrophotometric titration. Thus, an indirect probe was sought for confirming the origin of the observed p*K*.

Unlike the precursor tyrosine, the CT intermediate does have a readily discernible absorbance at 350 nm (*13*). Although the CT species is short-lived in WT apo-protein, we reasoned that if Y405 were being titrated in the pH profile shown in Figure 4, a corresponding effect from changing pH should be observed spectrophotometrically on the formation of the precursor tyrosine−Cu(II) complex. Indeed, at pH 8.6 (Figure 5A), the 350 nm absorbance accumulates to a visibly greater extent than at pH 7.0 (Figure 5B). The increase in absorbance at high pH may be due either to a higher extinction coefficient for the deprotonated vs protonated CT species or to a more favorable preequilibrium between liganded and unliganded Y405. These results support the assignment of the kinetically determined p*K* to the precursor tyrosine.

The observation of limiting rates at both high and low pH (Figure 4) is most consistent with a direct reaction between the CT complex and O_2 that limits the rate of TPQ formation and is dependent on the protonation state of the precursor tyrosine. Breakdown of the CT species is expected to proceed with a faster rate at high pH due to greater electron delocalization from the tyrosinate to copper and to the favorable change in redox potential that occurs upon tyrosine deprotonation [E_m for $TyrO^{\bullet}/TyrO^{-}$ (pH 11) is 0.2 V less than for $TyrO^{\bullet}$/TyrOH (pH 7) (*31*, *32*)].

The effect of solvent isotope on the rate of O_2 consumption was also investigated. Experiments of solvent isotope effects are expected to yield information regarding the presence of proton transfers during steps which are rate determining (*15*). The proposed rate-limiting reaction between the CT species and O_2 yields a peroxy adduct, which is expected to be stabilized by either concomitant proton transfer or electrostatic interactions. Solvent isotope effects help to discern these two possibilities; if there is accompanying proton transfer, a significant isotope effect will be observed, whereas the occurrence of electrostatic stabilization should result in a lack of an effect. Values for k_{bio} were obtained in deuterated buffers of varying pD (Figure 4); the value at high pD was 77.8 M^{-1} s^{-1} compared with 78.1 M^{-1} s^{-1} in protiated buffer, and at low, pD was 14.7 M^{-1} s^{-1} compared with 12.3 M^{-1} s^{-1} at low pH. The lack of a significant solvent isotope effect indicates that the proposed reaction between the CT species and oxygen is uncoupled from proton transfer.

Role of Active Site Residues in Biogenesis. Having elucidated many of the mechanistic details concerning the reaction between Y405 and O_2 during biogenesis, it was of interest to examine the effects of the consensus site sequence residues, which flank the precursor tyrosine in the apo-enzyme. These residues have previously been shown to play key structural roles in maintaining the proper orientation of TPQ during turnover (*18*). Thus, we predicted that if proper positioning of Y405 onto the copper were required for reaction with O_2 and if the consensus site residues play similar structural roles during biogenesis as catalysis, the rate

Scheme 2: New Proposed Biogenesis Mechanism Based on Kinetic Results[a]

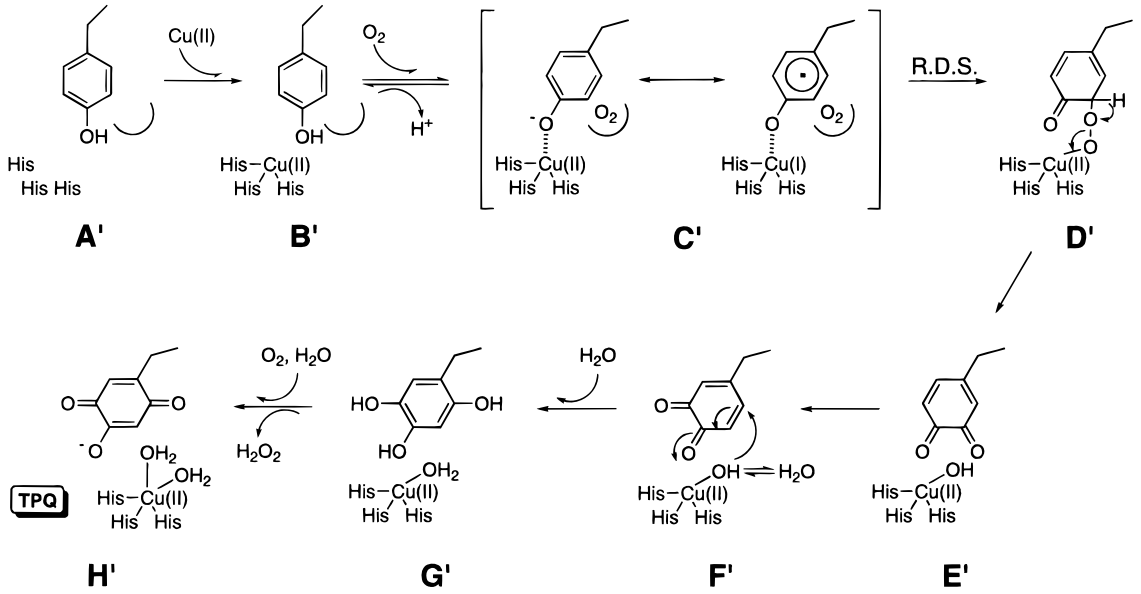

[a] R. D. S. indicates rate-determining step.

of oxygen consumption would be diminished in these mutants relative to WT apo-protein. Indeed, it was found that the rate of reaction with O_2 is reduced by 6-fold in E406Q and by greater than 30-fold in N404D (Table 1), supporting this argument. This structural role for the consensus site residues is also supported by spectroscopic results comparing E406Q and N404D with a mutant of the copper-binding site, H624C. Though all three mutants form TPQ at rates significantly diminished from WT protein (Table 1), only H624C was observed to readily form the precursor tyrosine-copper CT species (*13*).

The enthalpy of activation was also determined for O_2 consumption, by measuring the response in k_{bio} to temperature (Figure 6). It was found that the dependence on temperature was relatively small for WT protein, with a $\Delta H^{\ddagger} = 8.4$ kcal/mol calculated from the slope of the Arrhenius plot (Figure 6, inset). This is to be compared with a $\Delta H^{\ddagger}$ of 37.6 kcal/mol found previously for a mutant at the 404 position[3] (*18*). The origin of the large temperature in this mutant may be yet another consequence of its structural role in biogenesis, as the $\Delta H^{\ddagger}$ for H624C is much lower than for E406Q, similar to WT protein (unpublished results).

Mechanism of Biogenesis. On the basis of the kinetic results, a revised biogenesis mechanism is now proposed (Scheme 2). Copper binds rapidly to the enzyme (A′ → B′), though in the absence of O_2, it does not interact with Y405. Oxygen then binds in a site near the precursor tyrosine, displacing it onto the metal to form the CT species (B′ → C′). This movement is precisely modulated by the consensus site residues flanking the tyrosine and may be well represented by the Cu−OFF and Cu−ON forms seen crystallographically with the mature enzyme (*12*). The nature of the activated complex (C′) is best described as a tyrosinate−Cu(II) species, which has some tyrsosyl radical-Cu(I) character as a result of the covalency of the ligand−metal bond (*33*). A similar type of phenolate-metal interaction has been shown to occur in the iron-containing enzyme PCD (*34*); the possible mechanistic analogy between PCD catalysis and TPQ biogenesis was previously noted by Williams and Klinman (*35*), and is discussed in the preceding paper in this issue (*13*).

Formation of the CT complex activates Y405, which then reacts with O_2 to form the peroxy intermediate (C′ → D′), followed by subsequent conversion to DPQ (D′ → E′). Addition of water leads to reduced topa (G′), which is then reoxidized to yield the mature cofactor (H′); in this proposal, TPQ remains with the C-5 oxygen oriented toward the putative substrate channel, in accordance with the structure of mature HPAO (*36*) and mechanistic expectations. The kinetic data clearly indicate that a step concomitant with or preceding reaction of the first equivalent of O_2 is rate-limiting overall in this process, but is neither metal binding (A′ → B′) nor concomitant O_2 binding and CT complex formation (B′ → C′). This reasonably leaves either the reaction between the CT species and O_2 (C′ → D′) or an undetermined conformational change as possibilities for the rate-determining step in biogenesis. Several factors favor the former, rather than the latter. First, the observation and assignment of the pH effect directly to Y405 is more consistent with a rate enhancement when the CT complex consists of a deprotonated precursor tyrosine. Second, as previously mentioned, there appear to be no major conformational changes seen when comparing the apo- and holo-enzyme crystal structures of CAOs (*12*). Finally, the observation of a reduction in the rate of TPQ formation in the mutant H624C can be more easily rationalized with respect to changes in the electronic configuration of the CT species relative to WT HPAO, rather than by gross conformational changes of the active site.

This biogenesis proposal differs from previous mechanisms (Scheme 2 vs Scheme 1) on several key points. In particular, there is no evidence for a diffusional reaction between O_2 and Cu(I); rather, it is proposed that oxygen prebinds to the enzyme prior to reaction. Further, it is this binding of O_2 which triggers a reorientation of the precursor tyrosine onto the active-site copper that activates Y405 for a rate-limiting reaction with O_2. Importantly, the data presented herein and in the accompanying paper in this issue (*13*) provide the first

Scheme 3: Comparison of Initial Steps in TPQ Biogenesis and the Catalytic Oxidative Half-Reaction

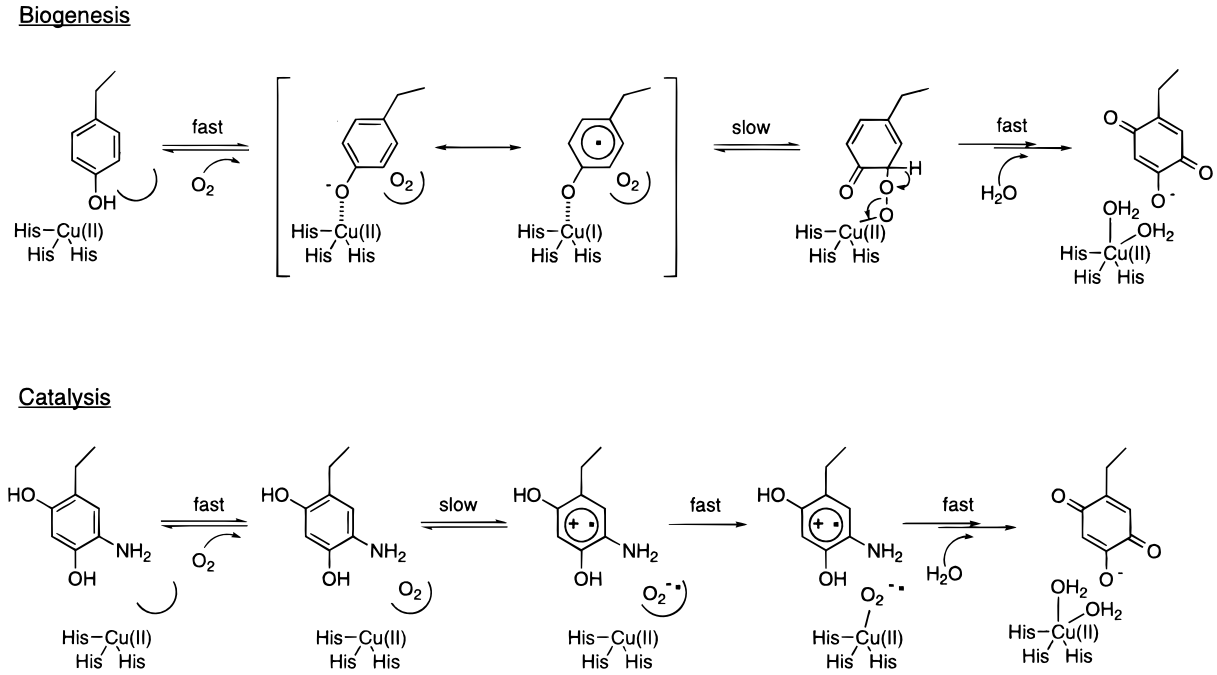

experimental evidence for an intermediate during TPQ biogenesis.

CAOs are unique in that they are able to catalyze efficiently the dual processes of TPQ biogenesis and turnover. Because enzyme active sites are typically envisioned as being structured to carry out a particular transformation, it is of general interest how the active site of HPAO achieves its diversity. At one extreme, it may be imagined that the active site is functionally partitioned, such that specific residues are utilized for biogenesis or catalysis, but not both. At the other extreme, an active site may be contemplated where a single set of residues and cofactors are used to catalyze both transformations, generating diversity through the ability to oxidize both the precursor tyrosine and reduced TPQ cofactor.

The relevance of these two possibilities in CAOs can be addressed by a general comparison of the mechanisms found in TPQ formation and turnover (Scheme 3). During both biogenesis and catalysis, oxygen is proposed to be prebound on the enzyme prior to undergoing reduction (*22*). In addition, the key structural contributions made by the consensus residues are similar in both processes. In these aspects, it appears that CAOs are well designed to make efficient use of their active-site elements in order to carry out their dual transformations.

However, the two mechanisms do contain important differences as well. Most significantly, during biogenesis the active-site copper plays an active role by promoting the reaction between the precursor tyrosine and oxygen. In contrast, during the oxidative half-reaction, the metal has been concluded to play an electrostatic role in the stabilization of superoxide formed during a rate-limiting electron transfer from reduced cofactor to O_2 (*22*, *37*). This mechanistic difference is presumably due to the much lower redox potential of the reduced aminoquinol compared with tyrosine; although E_m is not known for the semiquinone/aminoquinol couple, a value near 0.04 V (vs NHE) has been estimated for the analogous semiquinone/topa couple (pH ~8) compared with 0.74 V (vs NHE) for $TyrO^{\bullet}/TyrO^{-}$ (*32*, *38*). This difference in redox potential between aminoquinol and tyrosine can also account for the very large difference in second-order rate constants for biogenesis ($\sim 10\ M^{-1}\ s^{-1}$) vs catalysis ($\sim 10^5\ M^{-1}\ s^{-1}$) (*22*).

An interesting question which arises from the mechanisms of biogenesis and catalysis is the evolution of the active site of CAOs. An intriguing possibility is that the active site originally evolved to carry out oxidative chemistry on amines, but required an exogenous cofactor, such as pyrroloquinoline quinone (PQQ), for activity. At some later time, the oxidative chemistry previously developed to reoxidize the noncovalent redox cofactor was fortuitously applied to oxygenate a proximal tyrosine residue, creating TPQ. This evolved enzyme would be more advantageous in that it would avoid the need to obtain exogenous cofactors for activity. This scenario might account for the large K_m value found for O_2 during biogenesis; the kinetics of oxygen usage would not have been optimized for this "adapted activity", and further, the evolutionary pressure for the enzyme to attain a K_m nearer to typical physiological regimes would not be great, since formation of the cofactor simply needs to satisfy the physiological requirement of TPQ formation on a time scale compatible with the production of active protein.

The adapted ability to form modified amino acid cofactors may also be operative in other enzymes which catalyze oxidative reactions. The enzymes lysyl oxidase, galactose oxidase, and cytochrome *c* oxidase, all catalyze oxidative reactions and each contain a novel, oxidatively modified tyrosine as a redox cofactor (*39*−*42*).

CONCLUSIONS

A full kinetic analysis of O_2 utilization during TPQ biogenesis has been conducted, leading to a detailed proposal for the initial steps of cofactor formation. The effects of solvent viscosity, pH, solvent isotope, and temperature were

investigated and are consistent with oxygen binding to a specific site on the apo-enzyme prior to reaction with the precursor tyrosine. When combined with spectroscopic results (*13*), the kinetic data lead to a model in which binding of O_2 displaces the tyrosine onto the active-site copper. A subsequent reaction between the tyrosine−copper CT complex and O_2 is proposed to be rate limiting and is uncoupled from proton transfer.

This biogenesis mechanism has several features similar to that found for the catalytic oxidative half-reaction of CAOs, leading to the conclusion that this enzyme can initiate both biogenesis and catalysis utilizing common active-site elements. Future work will be directed at a more specific elucidation of the structural roles of the active-site mutants during biogenesis and turnover, through the use of detailed kinetics and crystallography.

ACKNOWLEDGMENT

The authors wish to thank Dr. Neal Williams for preliminary experiments.

REFERENCES

1. McIntire, W. S., and Hartmann, C. (1993) in *Principles and Applications of Quinoproteins* (Davidson, V. L., Ed.) pp 97−172, Marcel Dekker, Inc., New York.
2. Rea, G., Laurenzi, M., Tranquilli, E., D'Ovidio, R., Federico, R., and Angelini, R. (1998) *FEBS Lett. 437*, 177−182.
3. Salminen, T. A., Smith, D. J., Jalkanen, S., and Johnson, M. S. (1998) *Protein Eng. 11* (12), 1195−1204.
4. Howell, D. N., Valnickova, Z., Oury, T. D., Miller, S. E., Sanfilippo, F. P., and Enghild, J. J. (1998) *Mol. Vision 4*, 15−20.
5. Boomsma, F., van der Meiracker, A. H., Winkel, S., Aanstoot, H. J., Batstra, M. R., Man in't Veld, A. J., and Bruining, G. J. (1999) *Diabetologia 42*, 233−237.
6. Yu, P. H., and Zuo, D. M. (1997) *Diabetologia 40*, 1243−1250.
7. Janes, S. M., Mu, D., Wemmer, D., Smith, A. J., Kaur, S., Maltby, D., Burlingame, A. L., and Klinman, J. P. (1990) *Science 248*, 981−987.
8. Klinman, J. P. (1996) *Chem. Rev. 96*, 2541−2561.
9. Mu, D., Janes, S. M., Smith, A. J., Brown, D. E., Dooley, D. M., and Klinman, J. P. (1992) *J. Biol. Chem. 267* (12), 7979−7982.
10. Matsuzaki, R., Fukui, T., Sato, H., Ozaki, Y., and Tanizawa, K. (1994) *FEBS Lett. 351*, 360−364.
11. Cai, D., and Klinman, J. P. (1994) *Biochemistry 33*, 7647−7653.
12. Wilce, M. C. J., Dooley, D. M., Freeman, H. C., Guss, J. M., Matsunami, H., McIntire, W. S., Ruggiero, C. E., Tanizawa, K., and Yamaguchi, H. (1997) *Biochemistry 36*, 16116−16133.
13. Dove, J. E., Schwartz, B., Williams, N. K., and Klinman, J. P. (2000) *Biochemistry 39*, 3690−3698.
14. Cai, D., Williams, N. K., and Klinman, J. P. (1997) *J. Biol. Chem. 272*, 19277−19281.
15. Schowen, B., and Schowen, R. L. (1982) *Methods Enzymol. 87*, 551−606.
16. Fujisawa, H. (1990) *Methods Enzymol. 188*, 526−529.
17. Hevel, J. M., Mills, S. A., and Klinman, J. P. (1999) *Biochemistry 38*, 3683−3693.
18. Schwartz, B., Green, E. L., Sanders-Loehr, J., and Klinman, J. P. (1998) *Biochemistry 37*, 16591−16600.
19. Ruggiero, C. E., Smith, J. A., Tanizawa, K., and Dooley, D. M. (1997) *Biochemistry 36*, 1953−1959.
20. Mure, M., and Klinman, J. P. (1993) *J. Am. Chem. Soc. 115*, 7117−7127.
21. Su, Q., and Klinman, J. P. (1999) *Biochemistry 38*, 8572−8581.
22. Su, Q., and Klinman, J. P. (1998) *Biochemistry 37*, 12513−12525.
23. Ruggiero, C. E., and Dooley, D. M. (1999) *Biochemistry 38*, 2892−2898.
24. Fersht, A. (1985) *Enzyme Structure and Mechanism*, 2nd ed., pp 150−153, W. H. Freeman and Company, New York.
25. Northrop, D. B. (1998) *J. Chem. Educ. 75*, 1153−1157.
26. Brouwer, A. C., and Kirsch, J. F. (1982) *Biochemistry 21*, 1302−1307.
27. Frazee, R. W., Orville, A. M., Dolbeare, K. B., Yu, H., Ohlendorf, D. H., and Lipscomb, J. D. (1998) *Biochemistry 37*, 2131−2144.
28. Sorkin, D. L., Duong, D. K., and Miller, A.-F. (1997) *Biochemistry 36*, 8202−8208.
29. Grimshaw, C. E., Bohren, K. M., Lai, C.-J., and Gabbay, K. H. (1995) *Biochemistry 34*, 14374−14384.
30. Atkins, W. M., Wang, R. W., Bird, A. W., Newton, D. J., and Lu, A. Y. H. (1993) *J. Biol. Chem. 268*, 19188−19191.
31. DeFelippis, M. R., Murthy, C. P., Broitman, F., Weinraub, D., Faraggi, M., and Klapper, M. H. (1991) *J. Phys. Chem. 95*, 3416−3419.
32. DeFelippis, M. R., Murthy, C. P., Faraggi, M., and Klapper, M. H. (1989) *Biochemistry 28*, 4847−4853.
33. Cox, D. D., and Que, L., Jr. (1988) *J. Am. Chem. Soc. 110*, 8085−8092.
34. Orville, A. M., Lipscomb, J. D., and Ohlendorf, D. H. (1997) *Biochemistry 36*, 10052−10066.
35. Williams, N. K., and Klinman, J. P. (1999) *J. Mol. Catal. B: Enzymol. 326* (in press).
36. Li, R., Klinman, J. P., and Matthews, F. S. (1998) *Structure 6*, 293−307.
37. Mills, S. A., and Klinman, J. P. *J. Am. Chem. Soc.*, submitted.
38. Kano, K., Mori, T., Uno, B., Goto, M., and Ikeda, T. (1993) *Biochim. Biophys. Acta 1157*, 324−331.
39. Wang, S. X., Mure, M., Medzihradszky, K. F., Burlingame, A. L., Brown, D. E., Dooley, D. M., Smith, A. J., Kagan, H. M., and Klinman, J. P. (1996) *Science 273*, 1078−1084.
40. Ito, N., Phillips, S. E. V., Stevens, C., Ogel, Z. B., McPherson, M. J., Keen, J. N., Yadav, K. D. S., and Knowles, P. F. (1991) *Nature 350*, 87−90.
41. Ostermeier, C., Harrenga, A., Ermler, U., and Michel, H. (1997) *Proc. Natl. Acad. Sci. U.S.A. 94*, 10547−10553.
42. Yoshikawa, S., Shinzawa-Itoh, K., Nakashima, R., Yaono, R., Yamashita, E., Inoue, N., Yao, M., Fei, M. J., Libeu, C. P., Mizushima, T., Yamaguchi, H., Tomizaki, T., and Tsukihara, T. (1998) *Science 280*, 1723−1729.

BI9922244